

**Study Article**

# Frequency Adaptive Repetitive Control for Wind Power Applications using Grid Connected Inverter

**CH.CHERANRAJ**  
 B Tech Student  
 Dept of EEE  
 SVS Institute of Technology  
 Warangal, T.S, India

**P. GAJENDRACHARY**  
 B Tech Student  
 Dept of EEE  
 SVS Institute of Technology  
 Warangal, T.S, India

**B. NARESH**  
 B Tech Student  
 Dept of EEE  
 SVS Institute of Technology  
 Warangal, T.S, India

**D.PRASHANTH**  
 B Tech Student  
 Dept of EEE  
 SVS Institute of Technology  
 Warangal, T.S, India

**A.YAMUNA**  
 B Tech Student  
 Dept of EEE  
 SVS Institute of Technology  
 Warangal, T.S, India

**Abstract:** This paper presents a novel repetitive control for alternative energy generation systems (WPGS), which achieves best performance in steady-state conditions due to a variable sampling /switching amount technique. The main objective of VSPT is to get an range| number} number of samples per grid amount, which solves the main drawback of RC, i.e., the loss of rejection to periodic disturbances due to grid frequency drift. The sampling/switching frequency is adjusted with a variable sampling period filter phase-locked loop, which additionally adds lustiness to the system due to its inherent tolerance to grid voltage Distortion and unbalances, and events such as frequency steps and faults. The control subsystems are represented, designed, and verified experimentally in a 10-kW WPGS. The results obtained prove the accuracy of the proposed management even beneath severe disturbances, typical in grids with high WPGS penetration, providing ancillary functions to enhance reliableness and cut back operational prices.

**Keywords:-** Grid-Tie Current-Controlled Three-Phase Inverters; Power Quality; Repetitive Control;

## I. INTRODUCTION

WIND power generation systems (WPGS) play a key role in the distributed power generation scenario worldwide[1]. Modern variable-speed WPGS square measure connected to the grid through a current-controlled three-phase voltage source inverter (CC-VSI), as shown in Fig. 1. Phase currents injected to the grid must abide by with strict power quality standards, such as, which demand a total harmonic distortion (THD) of the injected currents below 5%. Given the increasing penetration of WPGS, even more strict limits square measure expected to be needed in the close to future. Moreover, new grid codes are requiring further options. Known as adjunct functions, they enhance robustness, safety, and reliability of the grid through reactive power injection, fault ride-through capabilities, compensation of harmonic currents generated by nearby nonlinear hundreds, and mitigation of asymmetrical loads, among others. A key part of a WPGS is that the CC-VSI current management and synchronism subsystems, which square measure entirely accountable for meeting all the aforementioned needs. This is a complex task considering the multiple disturbance sources affecting the system [1]. In addition to grid voltage fluctuations, unbalances and harmonics, inverter nonlinearities (e.g., dead times, voltage drops of semiconductor switches, inductance variations, etc.) are major causes of current distortion.

The power source represents the energy supplied by the wind generator. This control adds are sonant pole in the open-loop transfer function at the grid fundamental frequency,  $f_g$ , ensuring zero steady-state error at such frequency; grid phase/frequency information is implicit in the abc-dq transformation. However, inverter non linearities and unbalanced/distorted grid voltages generate errors not only at basic, but conjointly at harmonic frequencies of the grid. The limited open-loop information measure obtained with PI controllers results in low disturbance rejection capability and, hence, distorted line currents. An different methodology is to boost the steady-state performance of a classic current controller (proportional (P), dead-beat predictive (DBP), state feedback (SFB), etc.) by attaching a repetitive controller. Repetitive control (RC), which is based on the inner model principle has been employed in uninterrupted power provides active power filters power factor correction converters and the output active/reactive power of distributed power generation systems .In the plug-in scheme, the classic controller closes an inner loop providing fast response to grid disturbances and reference changes, while the RC ensures zero steady-state error by placing resonant poles at fundamental and each harmonic frequency of the grid up to the Nyquist frequency. This paper proposes an different answer, which consists in changing  $f_s$  adaptively thus  $f_s = N f_g$ , where N is a fixed whole {number |number} number [2].

## II. CONTROL STRUCTURE AND PRINCIPLES

The WPGS control system is discovered in Fig. 1, where the VSPF-PLL output governs the sampling/switching period value,  $T_s = 1/f_s$ , which feeds the pulse width modulator (PWM). This in turn generates the start-of-conversion signal for the analog-to-digital converters (ADCs). Thus, the whole system operates with a frequency  $f_s$  that is a definite multiple of  $f_g$ ,  $f_s = N f_g$ . During traditional operation, grid frequency drifts are tiny (e.g., =2%), so  $f_s$  keeps shut to its nominal value. As a consequence, the variation over time in the spectral content

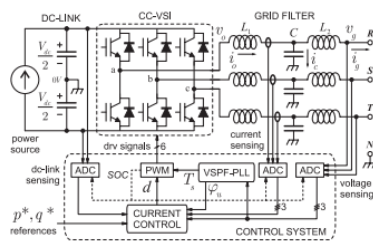


**Fig. 1. Block diagram of the proposed control system within a CC-VSI for WPGS application.**

## Study Article

due to  $f_s$  is negligible, hence switch losses area unit approximately the same and therefore the grid filter style is left unchanged.

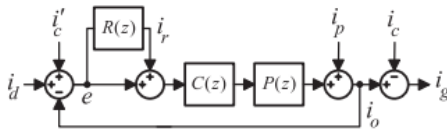


Fig. 2. Block diagram of the control system.

### A. Current Control

A block diagram of the control structure adopted is shown in Fig. 2. Due to the VSPT, the sampling time  $T_s$  follows the grid period  $T_g$ , which changes slowly. This small and slow drift allows to treat the variable-time separate system of Fig. 2 as a fixed-time one with negligible error [29]. A further discussion and stability analysis due to the variable sampling frequency is performed in Section IV-E.  $P(z)$  is the plant transfer function comprised by the modulator, the inverter, the LCL filter, and the grid. Signal  $i_g$  is the current injected into the grid,  $i_o$  is the inverter output current, and  $i_c$  is the capacitor current. Notice from Fig. 1 that  $i_d = i_o - i_c$ . In Fig. 2,  $i_d$  is the reference (desired) current. Since only  $i_o$  is measured,  $i_g$  can solely follow  $i_d$  if  $i_c$  is effectively stipendiary by the feed forward term  $i_c$ , which is additional to  $i_d$ [3]. The exogenous signal  $i_p$  represents the multiple disturbances affecting the output current: grid voltages not completely canceled by feed forward techniques and inverter nonlinearities such as dead times, among others.

### B. Comparison With Other Rc Approaches

An vital downside of RC is its gain loss once the grid frequency varies, which, in turn, reduces the control loop disturbance rejection and reference tracking capability [20]. This occurs as a result of the order  $N$  of the RC isn't capable the ratio  $T_g/T_s$ , and hence the RC poles no longer lie at multiples of  $f_g$ . Several approaches have been projected within the literature to deal with this issue, the most common being the introduction of a fictitious sampler operator. A recent and more refined approach uses associate degree FIR filter with variable within the RC algorithmic program to emulate the divisional delay produced by the frequency drift. A similar approach is found in [20] which employs a straightforward first-order low-pass filter, cascaded with the RC delay line, with adjustable cutout frequency. In the proposed strategy, the VSPT allows the use of the easy RC algorithm (3) consisting of a delay and simple filters in  $Q(z)$  and  $L(z)$  (which are conferred in detail in Section IV), where the same numerical errors are nonexistent since all the coefficients are one or powers of two. An vital downside of RC is its gain loss once the grid frequency varies, which, in turn, reduces the control loop disturbance rejection and reference tracking capability. This occurs as a result of the order  $N$  of the RC isn't capable the ratio  $T_g/T_s$ , and hence the RC poles no longer lie at multiples of  $f_g$ . Several approaches have been projected within the literature to deal with this issue, the most common being the introduction of a fictitious sampler operator. A recent and more refined approach uses associate degree FIR filter with variable coefficients within the RC algorithmic program to emulate the divisional delay produced by the frequency drift.

### III. DYNAMIC MODEL FOR STABILITY ANALYSIS

This section develops a new discrete-time system model, sampled at frequency  $f_g$ , derived from the original model sampled at  $f_s$ . The new model enables a simple analysis of system stability and dynamics. First, it is assumed that  $f_s$  has been stabilized and therefore a fastened magnitude relation  $N = T_g/T_s$  has been achieved. The tracking error signals with and while not the RC are  $e(kT_s)$  and  $b(kT_s)$ , as defined in (5) and (4), respectively. If time is split in slots of duration  $T_g$ , these signals can be expressed as

$$b(kT_s) = \sum_{i=-\infty}^{\infty} b_i(kT_s)$$

$$e(kT_s) = \sum_{i=-\infty}^{\infty} e_i(kT_s)$$

### IV. CONTROL SYSTEM DESIGN

The control and synchronicity sub systems area unit designed taken an example case of a WPGS whose main parameters area unit listed in Table I, which correspond to the experimental epitome employed in Section V. To control every section severally to allow the injection of asymmetrical currents, the VSI has the neutral point of the load connected to the dc link, as shown in Fig. 1. As a consequence, the inverter driving signals area unit generated by three freelance PWM modulators, and the control is ideally developed in the natural arrangement (abc coordinates) [4]. Nevertheless, it is worth mentioning that the proposed management and methodology area unit valid for any reference frame (abc,  $\alpha\beta$ , and dq), as pointed out in Section I.

#### A. Inner Loop Design

The first step in coming up with the system is to get a model for  $P(z)$  and to close a stable and quick internal loop with  $C(z)$ . A discrete-time model for the plant, considering the modulator reference duty cycle  $D(z)$  and current  $I_o(z)$  as the input and output variables, is presented in [1].

#### B. RC Design

Section III showed that optimum results are achieved if the inner loop dynamics is completely canceled, which is achieved with  $L(z) = 1/H(z)$ . Nonetheless, due to plant uncertainties and parameter variations, achieving this task is not trivial. Another, more sensible approach is to solely compensate section shifts in the frequency regions where stability is compromised. Notice that  $H(\omega) \sim 1$  for frequencies below the inner loop crossover frequency, so adopting the crossover frequency, the magnitude of  $H(\omega)$  decreases and its phase rotates negatively, so the issue  $1 - L(\omega)H(\omega)$  in (6) could be  $> 1$  (unstable system). To compensate this phase shift, the following linear phase-lead compensator is employed. An optimum worth of  $m$  is obtained with the aid of Fig. 5, which plots  $|a(\omega)|$  for many values of  $m$  in. Fig. 5(a) is for  $Q(z) = 1$ , and it can be determined that for any  $m, |a(\omega)| > 1$  (or terribly shut to one) within the high-frequency vary, so the system is often unstable. The curves in Fig. 5(b) were obtained for  $Q(z)$  as, and show that the system is stable for  $m > 2$ . Notice how the curve peak lowers with sequent increments of  $m$  until  $m = 4$ , after that peaks begin to rise. Hence, the optimum value for this system is  $m = 4$ . Fig. 6 plots step responses for the error  $e(kT_s)$  to illustrate the effect that the

## Study Article

selected alphabetic character and L filters wear the system stability. Fig. 6(a) shows the case for  $Q(z) = L(z) = 1$ , showing that the system is unstable, as shown by Fig. 5. Fig. 6(b) shows the case for the selected filters (19) and (21), showing a stable system [5].

### C. PLL Design

The proposed compensator used to shut the PLL in the cited work has two zeros, a pole in  $z = 1$  and again for stability functions. In addition, this transfer function favors the settling time at Associate in Nursing expense of quick fluctuations in the sampling period throughout transients. However, to provide an adequate performance for the RC, the following simpler transfer function is adopted.

### D. Capacitor Current Feed Forward Cancellation

As shown in Figs. 1 and 2, the injected current  $i_g$  can follow  $i_d$  only if the feed forward term effectively compensates the capacitor current  $i_c$ . This is mainly obligatory by the grid voltage, i.e.,  $i_c \sim Cdv_g/dt$ . Hence, grid voltage harmonics will turn out harmonic currents through C, increasing  $i_g$  distortion. The feed forward compensation term is calculated as

$$i'_c(k) = \frac{C}{T_s} (v_g(k) - v_g(k-1))$$

### E. Stability Analysis Under Variable Sampling Frequency

Rather than employing the strong management approach projected for stability analysis under variable sampling frequency, a more simple and easier-to-apply technique is presented in the following. Grid frequency variations overtime may occur among many seconds at worst [34], while the RC response in closed loop is within some grid cycles. Hence, the whole system may be treated as a quasi-static one meaning that the dynamic models remain the same, with  $T_s$  acting only as a slowly varied parameter. It can be discovered that  $T_s$  is just gift within the plant model  $P(z)$  where the issue  $T_s/L_s$  affects both its gain and the pole location at  $z = e^{-R_s T_s/L_s}$ . Fig. 7 shows a set of plots for  $|a(?)|$  (as in Fig. 5 however with  $m = 4$ ), for different values of  $(T_s/L_s)_{\text{norm}}$  (normalized to nominal value), defined as the quantitative relation between a nominative  $T_s/L_s$  and also the nominal  $(T_s/L_s)_{\text{nom}} = 0.05$  s/H (according to Table I). Plots in Fig. 7(a) are for  $(T_s/L_s)_{\text{norm}} = \text{one}$ , where it will be detected that the system is always stable.

## V. PROPOSAL VALIDATION

### A. Experimental Setup

The proposed management was through an experiment tested to assess both its steady-state and dynamic performances in a tiny urban WPGS, shown in Fig. 8 (left). This H-rotor type windturbine is appropriate for locations with structural limitations and low-weight low cost necessities. The WPGS is coupled to the grid through a three-phase four-wire grid-connected VSI (Fig. 1). The experimental prototype is shown in Fig. 8 (right). The main system parameters are listed in Table I. The inverter switches are enforced with Semikron SKM75GB176DIG BTs for improved ruggedness. The configured dead time for these switches is 2.5  $\mu$ s, which ensures safe operation condition. On the other aspect, such high dead times (2.5% of  $T_s$ ) have a noticeable impact on the output currents

. The digital control framework is composed of a custom board based on a TX Instruments' microcontroller ( $\mu$ C)TMS320F28335, which is a progressive device extremely employed in power applications. All the control algorithms were implemented victimization 32-bit floating-point arithmetics. The 12-bit ADCs integrated onto the  $\mu$ C chip was used to sample all the control variables. A 16-bit enhanced digital 3PH-PWM (ePWM) module was employed to drive the power stage. To implement the variable sampling/switching frequency technique, the ePWM was configured to update its amount and duty cycle with the new values only once the current amount ends, ensuring the correct operation of management algorithms. This is possible as a result of the ePWM options special buffer registers, which will be written at any time with the new values. An interrupt at the beginning of every PWM amount synchronizes each control tasks and AD conversions. Notice that neither complex hardware nor additional package is needed to implement a variable sampling/switching frequency.

### B. Steady-State Performance

The projected control is compared against alternative proposals: a sturdy prophetic current controller (RPCC) presented and a classical PR controller with harmonic compensation (PR + HC) (harmonic orders:  $n = 3, 5, 7, 9, 11$ ). A sinusoidal current reference  $i_d$  of 20 A peaks synchronal with the positive sequence of the grid was generated to inject 9.3 kilowatt of active power. The feed forward term (24) was added to compensate the undesired LCL-filter electrical condenser current, as in Fig. 2. The grid phase voltage  $v_g$  is additionally shown, which exhibited high harmonic content ( $\text{THD}_v = 4.8\%$ ) as expected for a weak urban grid.

### C. Power Transient Performance

Power flow adjustment in the grid-connected VSI of a WPGS is not only vital however conjointly a demand of the many standards that focus on integrating energies from renewable sources into the grid. Fast following of the active power flow ensures extracting most power from gusts in tiny urban wind generators and minimizes the energy storage requirements among the WPGS [3]. Fast following of reactive power flow is required to cut back grid voltage variations in the point of common coupling throughout wind generation fluctuations or connection/disconnection of nearby serious masses.

### D. Frequency Transient Performance

Grid frequency variations become more vital as the amount of grid-connected WPGS will increase. Indeed, some of the standards address this issue, and request the WPGS to remain connected even beneath massive frequency changes ( $\pm 6\%$ ) during some minutes (fault ride-through capability).

A series of tests was conducted to assess the performance of the RC under frequency variations.

### E. Performance Under Grid Disturbances And Faults

Simulations were carried out to assess the system performance under severe grid faults and voltage unbalances. Experimental tests could not be conducted as a result of no means that to generate such conditions during a safe manner were available at our research laboratory. Accurate simulation models were employed matching the

## Study Article

system parameters of Table I. Comparative tests combining RC with the standard SRFPLL and VSPF-PLL are shown in Fig. 12. Grid phase voltages ( $v_{ga}$ ,  $v_{gb}$ , and  $v_{gc}$ ) are balanced and while not distortion before  $t_0$ . A high distortion is applied to these voltages ( $THD_v = 11.2\%$ ) from  $t_0$  onward, as shown in Fig. 12(a). Then, a grid fault is applied on  $t_1$ : phase a is short circuited to ground ( $v_{ga} = 0$ ), while  $v_{gb}$  and  $v_{gc}$  rise in magnitude and their phases rotate to be  $180^\circ$  from each different.

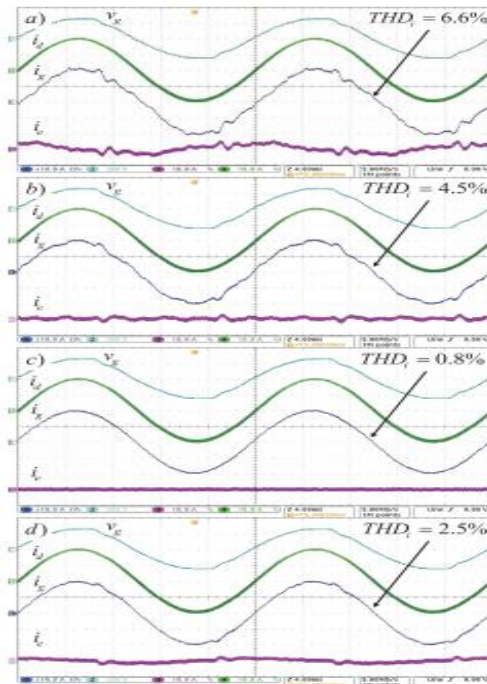


**Fig. 4 Steady-state performance injecting 20 A peak per phase. (a) RPCC. (b) PR + HC. (c) Proposed RC. (d) Proposed RC without capacitor current feedforward compensation**

## VI. CONCLUSION

An RC for WPGS was bestowed, which achieves best performance in steady-state conditions due to a VSPT. With this new control strategy, the loss of rejection due to grid frequency drift is corrected, as proven by the experimental results. The sampling/switching frequency is slightly adjusted around 10 kilohertz with a VSPF-PLL, which conjointly adds hardness to the system due to its inherent tolerance to grid voltage distortion.

Computational times in a state-of-the-art DSP were concerning V-day of a bearing amount of  $100 \mu s$ , which includes RC and PLL algorithms, proving that the solution is computationally economical. The implementation of the variable frequency sampling is straightforward because it solely requires a few customary hardware modules (configurable ADC and PWMs), which are already embedded in the selected DSP. The proposed RC was compared through the experimental tests to other management strategies: AN RPCC and a PR + HC. The tests showed the superiority of the method:  $THD_i = 6.6\%$  and computational price of  $11 \mu s$  for the RPCC,  $THD_i = 4.5\%$  and  $18 \mu s$  for the PR + HC, and finally  $THD_i = 0.8\%$  and fifteen  $\mu s$  for the RC.

## VII. REFERENCES

- [1]. C. Busada, S. Gomez Jorge, A. Leon, and J. Solsona, "Current controller based on reduced order generalized integrators for distributed generations systems," IEEE Trans. Ind. Electron., vol. 59, no. 7, pp. 2898–2909, Jul. 2012.
- [2]. F. Gonzalez-Espin, G. Garcera, I. Patrao, and E. Figueres, "An adaptive control system for three-phase photovoltaic inverters working in a polluted and variable frequency electric grid," IEEE Trans. Power Electron., vol. 27, no. 10, pp. 4248–4261, Oct. 2012.
- [3]. E. ON Netz GmbH, "Grid connections regulations to high and extra high voltage," Tech. Rep., Apr. 2006.
- [4]. J. Espi Huerta, J. Castello-Moreno, J. Fischer, and R. Garcia-Gil, "Asynchronous reference frame robust predictive current control for three-phase grid-connected inverters," IEEE Trans. Ind. Electron., vol. 57, no. 3, pp. 954–962, Mar. 2010.
- [5]. V. Kaura and V. Blasko, "Operation of a phase locked loop system under distorted utility conditions," IEEE Trans. Ind. Appl., vol. 33, no. 1, pp. 58–63, Jan./Feb. 1997.